# Grazing-incidence small-angle X-ray scattering study of porous dielectrics used in advanced microelectronic interconnections

**Jean-Paul Simon,[a]\* Vincent Jousseaume[b] and Guy Rolland[b]**

[a]CNRS-INPG-UJF Grenoble, France, and [b]LETI/CEA Grenoble, France. Correspondence e-mail: jean-paul.simon@ltpcm.inpg.fr

The increase of the integration density and of the operation speed in ultra-large-scale integrated microelectronics requires a reduction in the dielectric constant for high-frequency insulation between the copper connections of some tenth-of-micrometre thickness. Recently, the quality of the dielectric has been defined by its dielectric constant $k$ (>1) relative to the unpolarized vacuum ($k = 1$). Bulk low $k$ will never reach $k$ lower than 3 and the only way to achieve a further decrease in $k$ is to introduce nanoporous dielectric films compatible with the required mechanical behaviour. We compare the merits and the structure determined by grazing-incidence small-angle X-ray scattering (GISAXS) of four different growth processes: plasma-enhanced chemical vapour deposition or spin coating with three variants: dual-phase blend, self-assembled approach, nanoclustering precursor. All of them are baked in order to cure the amorphous $Si_wO_xC_yH_z$ 'skeleton' (SiOCH). Depending on the process used, the pore morphologies are very different. They range from well defined pores of 4–5 nm diameter to sub-nanometric ill-defined pores which may be described as density fluctuations. Finally, it appears that the curing process is a key problem, which up to now has been difficult to characterize by GISAXS.

## 1. Introduction

Low-$k$ dielectric materials are widely used as the insulating material between interconnects in semiconductors. They reduce interconnect parasitic capacitance and decrease power consumption. The increase of the integration density and of the operation speed of ultra-large-scale integrated (ULSI) devices require ultra-low-$k$ materials with a $k$ value of less than 2.4 for the 45 nm technology node. Bulk low-$k$ materials integrated in devices and prepared by plasma-enhanced chemical vapour deposition (PECVD) have $k$ values larger than 3. To decrease $k$ further, pores are introduced in order to achieve the ultra-low dielectric constant required. Pores have to be of a nanometric size in order to be compatible with the small feature sizes of Cu–ultra-low-$k$ (ULK) interconnections. Among all the ULK materials, porous SiOCH is the most mature for potential integration. Several deposition techniques can be carried out: spin-coating or PECVD, all of them followed by a thermal treatment for cross-linking and/or porogen removal. Different strategies can be used to create pores in an amorphous SiOCH matrix:

(a) The first technique, SC-Po, consists of depositing, by spin-coating, a dual-phase thin film using two precursors: a methylsilsesquioxane for the matrix and a sacrificial organic molecule (porogen approach). The porogen is degraded during a subsequent thermal treatment. Two nanoparticle polymers have been used in this work, Po1 and Po2.

(b) This approach can also be performed by PECVD using an organosilane precursor for the matrix and different organic molecules as the porogens. In the four presented cases the skeleton remains the same but samples differ by the sacrificed porogen and by the final treatment (to degrade the porogens and to cross-link the skeleton): simple thermal, or electron beam or ultra-violet assisted. The final treatment should allow a total elimination of the porogen to create porosity and a good cross-linking of the skeleton for appropriate mechanical properties.

(c) The third method (SC-SA) consists of using self-assembling polymer technology, the porosity being created during the cross-linking process with a thermal treatment.

(d) The fourth method (SC-NC) is based on nanoclustering silica precursors.

The mechanical and dielectric properties are, of course, fundamental, but there is a need to characterize the structure at the nanoscale. Grazing-incidence small-angle X-ray scattering (GISAXS) is a technique of choice since it can determine patterns, pore sizes, spatial distribution of pores and eventual anisotropy. There are few published data (Hsu *et al.*, 2000; Kawamura *et al.*, 2001; Huang *et al.*, 2002) and the most complete correlation between chemistry and structure by GISAXS known to the authors has been given by Lee *et al.* (2005).

In this work, we analyze GISAXS patterns from eight samples, four of them prepared by spin-coating, four by PECVD with different thermal treatments. It has been verified that GISAXS signals in the different samples were almost negligible before the curing treatment: the porogen and the matrix have very close electronic densities. We show that the correlation between structure and properties is not direct: the final annealing step is a key problem.

The films were also characterized using Fourier transform infrared spectroscopy (FTIR) which measured peaks that are characteristic of skeleton bonds. The volume fraction of pores can be deduced from X-

ray reflectivity (XRR), assuming that the skeleton is identical to the bulk skeleton. This volume fraction was also estimated using porosimetry ellipsometry (EP) coupled with solvent adsorption. Pore sizes and their size distribution can also be evaluated after correction for the surface layer physi-sorption.

## 2. Experiments

Small-angle scattering is well adapted to two-phase materials, skeleton and pores; GISAXS is mandatory since the buffer of the Si wafer is opaque and, if it is thinned down to ~80 μm, the ULK layer is too thin (~300 nm) to provide a tractable signal. GISAXS multiplies this signal by a factor of ~200 at 0.3°, but the beam size should not exceed 100 μm and thus requires a synchrotron experiment. Results have been obtained on the beamline 'Diffraction diffusion anomale multilongueur d'onde' (D2AM) of the European Synchrotron Radiation Facility with a photon flux of ~5 × $10^{10}$ photons s$^{-1}$, using an adaptation of the SAXS camera in order to ensure grazing incidence, the whole bench being under vacuum. Two-dimensional images (above the shadow of the sample) were recorded by a low-noise 16-bit charge-coupled-device camera (Fig. 1). Data correction and reduction will be described in Jousseaume *et al.* (2007). With the height of the beam being smaller than 0.1 mm and the samples being 70 mm long, the foot-print of the beam was completely on the sample. Therefore for different grazing incidences $\alpha$ (above 0.22°, the critical angle of the Si wafer at 8 keV), the signal *versus* the norm of the scattering vector $q$ [$q = 4\pi\sin(\theta)/\lambda$, where $\theta$ is half the angle between the incident and scattered beam and $\lambda$ the photon wavelength] is homothetic in a ratio of the volume probed, *i.e.* in $1/\alpha$ (Fig. 2). Below $\alpha_{c\,Si}$, the GISAXS signal is stronger: GISAXS is triggered by the incident and the strong-reflected beams.

## 3. Results and discussion

Fig. 1 shows typical GISAXS images; they are isotropic for the SC-Po2 and SC-SA samples. Let us notice that the two dimensional image of SC-Po2 (Fig. 1a) presents a well defined ring of maxima, which is also illustrated on Fig. 2: it means that there is a narrow distribution of sizes and a fairly well organized pattern of pores with a narrow distribution of the mean distances between pores, ~8.5 nm. A slight anisotropy appears for SC-NC in the horizontal direction ($q_y$) with correlation distances $2\pi/q_{y\,max}$ of 6.5 nm. For three PECVD samples composed of the same matrix and different
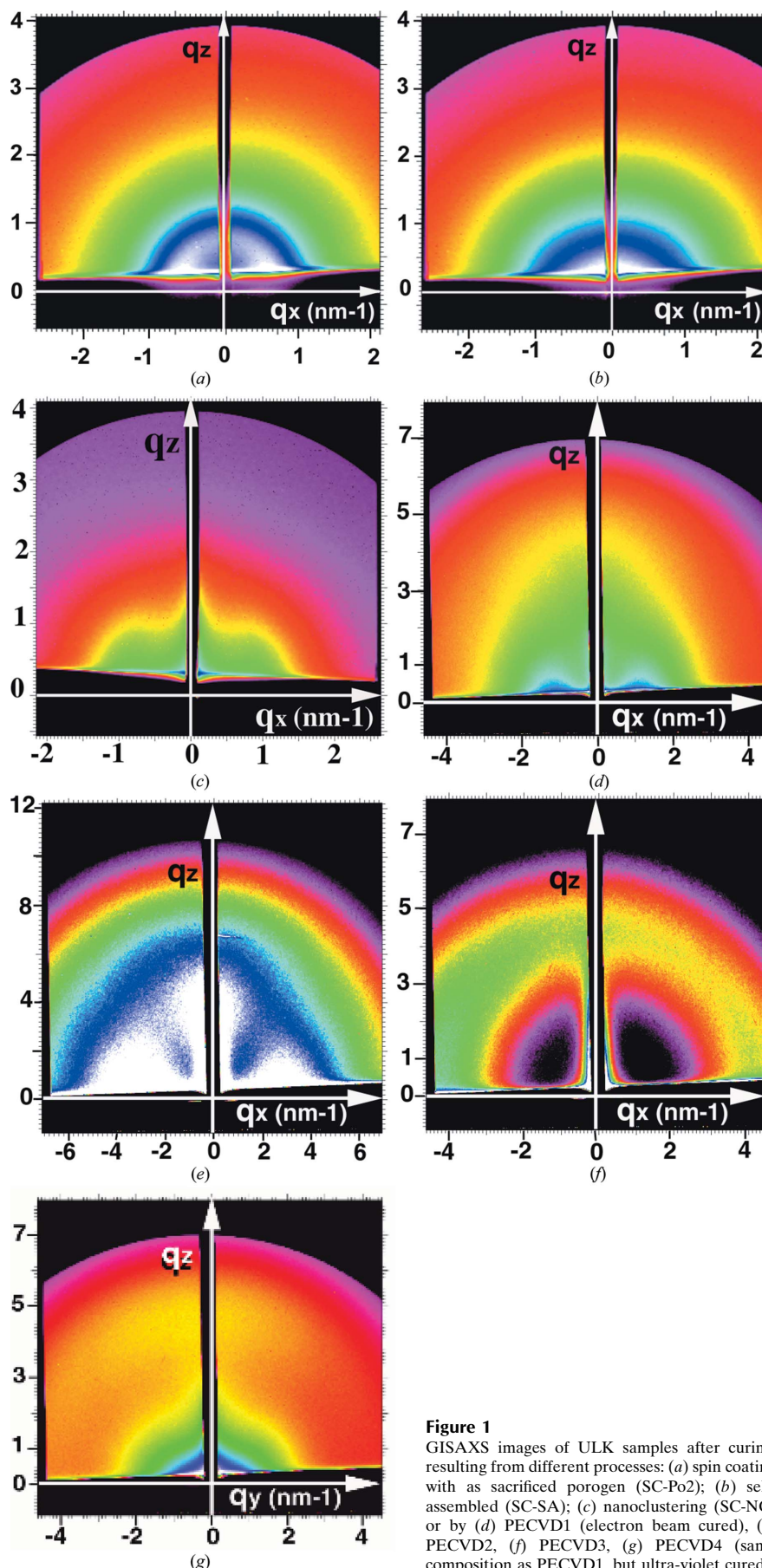


**Figure 1**
GISAXS images of ULK samples after curing, resulting from different processes: (*a*) spin coating with as sacrificed porogen (SC-Po2); (*b*) self-assembled (SC-SA); (*c*) nanoclustering (SC-NC) or by (*d*) PECVD1 (electron beam cured), (*e*) PECVD2, (*f*) PECVD3, (*g*) PECVD4 (same composition as PECVD1, but ultra-violet cured).

**Table 1**
Dielectric constant, elastic modulus, pore volume fraction as determined by XRR and EP.

Precision on $k$ is ±0.05, on the modulus ±20% and on $f$ ±0.5%; reminding the assumptions given in the text.

| | $k$ | Modulus (GPa) | $f$ (%) (XRR) | $f$ (%) (EP) |
|---|---|---|---|---|
| SC-Po1 standard | 2.2/2.1 | 2 to 4 | 43 | 43.5 |
| SC-Po2 monodisperse | 2.2 | 2 | 40 | 38 |
| SC-SA | 2.2 | 3.5 | 43 | 41 |
| SC-NC | 2.35 | 5 | 38.5 | 38 |
| PECVD1 (e-beam) | 2.55 | 6.5 | – | 24 |
| PECVD2 | 2.3 | 3 | – | 30 |
| PECVD3 | – | – | – | – |
| PECVD4 (UV) | 2.6 | 4.5 | – | 24 |

**Table 2**
Sizes and mean distances between pores ($h$ for horizontal, $v$ for vertical correlations), as given by GISAXS and by EP.

Precision on the size is better than 10%.

| | $\phi_{Iqm2}$ (nm) | $\phi_{absorb}$ (nm) | $\delta\phi_{absorb}$ (nm) | $d = 2\pi/q_m$ (nm) |
|---|---|---|---|---|
| SC-Po1 standard | 4 | 3.0 | 1.0 | 10 |
| SC-Po2 monodisperse | 5 | 5.5 | 2 | 8.5 |
| SC-SA | 4/5 | 3 | −1/+2 | >12 |
| SC-NC | 3.5 | 2 | ±1 | ($h$) 6.5 |
| PECVD1 (e-beam) | – | 2 | ±1 | ($h$) 3.5 |
| PECVD2 | 0.6 | 2 | ±1 | ($v$ and $h$) 1.75 nm |
| PECVD3 | 0.6 | – | – | (isotropic) 1.6 nm |
| PECVD4 (UV) | – | 2.2 | ±1 | (weak $v$ and $h$) |

kinds of porogens, the signal is much weaker; moreover the images are completely different. In PECVD1, at larger angles, *i.e.* at higher $q$, a strong horizontal correlation is observed with correlation distances of 3.5 nm. In PECVD2, there is both a horizontal (mean distance of 1.75 nm) and a vertical correlation (mean distance of 1.6 nm) as if pores were assembled in an almost 'pseudo-cubic' lattice. In PECVD3, there is a well defined isotropic ring with very small correlation distances (1.6 nm). Finally, in PECVD4, it appears as a slight reinforcement on the ring in the $q_z$ direction which evidences a slight anisotropy.

Radial averages were made in the −45 to 45° quadrant (Fig. 3). It appears that the asymptotic law $q^{-n}$ was between 3 and 3.5 in the intermediate $q$ range and can drop to $n = 2$ in the 4 to 6 nm$^{-1}$ range. This is in contradiction with pores with abrupt interfaces ($q^{-4}$ Porod's law) and may be interpreted in term of fractals, and/or, for $n = 2$, in terms of density fluctuations.

Moreover, XRR and ellipsometry have shown that the pore volume fraction is above the percolation threshold (Table 1).

Therefore, a classical analysis in terms of spherical pores will only give the order of magnitude of the pore size. First a Guinier's regime is always checked. In almost all the samples (except SC-Po2, which is not a common feature of the different sacrificed porogens), no Guinier's range is found and an analysis using a lognormal distribution of spheres leads to a scheme where the width of the distribution is larger than the mean size: with these values, the model is insig-
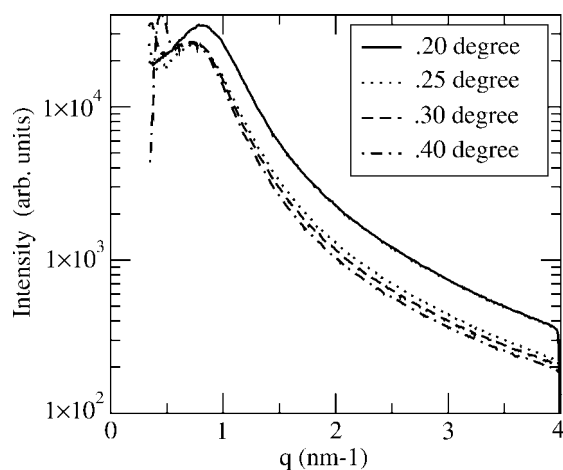
nificant. Therefore we prefer to use the concept of pores having the largest contribution to the volume fraction, *i.e.* the maximum of the plot $Iq^2$ versus $q$. With spherical pores, the diameter is equal to $2(5)^{1/2}/q_{Iq^2_{max}}$. Results are gathered in Table 2 and are compared to EP data. The same trends appear in both techniques, although sizes deduced from EP are generally smaller than GISAXS sizes. SC-Po2 has the largest (4 to 5 nm) and the PECVDs the smallest, below 1 nm; in this case, the terminology of 'density fluctuation' would have more physical basis than pores. The asymptotic law of $q^{-2}$ also supports this description. Finally, we remark that, in SP-NC, the sizes deduced by EP are of the order of 2 nm while sizes deduced by GISAXS are 4 nm: this opens the question about the open porosimetry which may be a fraction of the whole.

The volume fraction could in principle be extracted from the integrated intensity ($\int Iq^2 \mathrm{d}q$), but the extrapolation part at large $q$ is uncertain and the value, varying as $f(1–f)$, is weakly dependent on the volume fraction $f$ in the range 30–50%. They have no big difference being close to 40% while the dielectric constant ($k$) as well as the elastic modulus may differ largely (Table 1).

It appears that the dielectric and mechanical properties are very sensitive to the curing process associated with the final thermal treatment. For instance, for PECVD with the same blend, assisted by e-beam (Fig. 2*d*) or by UV illumination (Fig. 2*g*), the GISAXS patterns are very different.
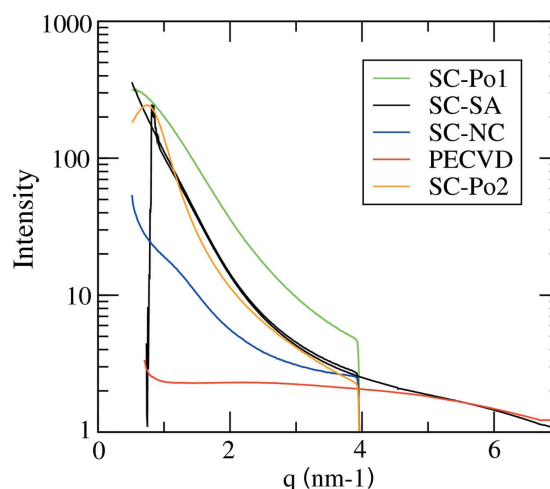


**Figure 2**
Radial distribution of the GISAXS intensity for sample SP-Po2 (corresponding to the image, Fig. 1*a*) as function of the grazing angle.



**Figure 3**
Radial distribution of GISAXS intensity for samples presented in Fig. 2 (PECVD is PECVD1), plus the optimized SP-Po1.

## 4. Conclusion

We have shown that GISAXS gives the most complete description of the morphology and patterns of pores in the ultra-low-$k$ dielectrics, materials which are nowadays evaluated for the 65 nm ULSI technology. The sizes of PECVD pores are so small, less than a nanometre, that a description in free volume may be more appropriate. For other samples, the size is of the order of several nanometres. In all cases, it is worthwhile to cross-check these results with the complementary techniques, FTIR, XRR and EP. Finally, the influence of the final treatment (annealing assisted or not, by UV or e-beam) is not fully understood both as morphology and mechanical properties. More studies are needed.

## References

Huang, E., Toney, M. F., Volksen, W., Mecerreyes, D., Brock, P., Kim, H.-C., Hawker, C. J., Hedrick, L. F., Lee, V. Y., Magbitan T. & Miller R. D. (2002). *Appl. Phys. Lett*, **81**, 2232–2234.

Hsu, C.-H., Lee, H.-Y., Liang, K. S., Jeng, U.-S., Windover, D., Lu, T.-M. & Jin, C. (2000). *Mater. Res. Soc. Symp. Proc.* **612**, D5.23.

Jousseaume, V., Rolland, G., Babonneau, D. & Simon J.-P. (2007). *J. Appl. Phys.* Submitted.

Kawamura, S., Maekawa., K, Ohta, T., Omote, K., Suzuki, R., Ohdaira, T., Tachibana, M. & Suzuki, K. (2001). *Proceedings of the International Interconnect Technology Conference*, 4–6 June 2001, Burlingame, Canada, pp. 195–197. Piscataway, NJ: IEEE.

Lee, B., Park, Y.-H., Hwang, Y.-T., Oh, W., Yoon, J. & Ree, M. (2005). *Nat. Mater.* **4**, 147–150.